THE SPECTRUM OF RATE CONTROLLING DEFORMATION MECHANISMS OPERATING IN CREEP IN AN Al-8.5Fe-1.3V-1.7Si-15SiC$_p$ COMPOSITE AT TEMPERATURES RANGING FROM 623 TO 948 K

JOSEF ČADEK[1]*, KVĚTA KUCHAŘOVÁ[1], SHIJIE ZHU[2]

Creep in an Al-8.5Fe-1.3V-1.7Si alloy reinforced with silicon carbide particulates – an Al-8.5Fe-1.3V-1.7Si-15SiC$_p$ composite – is investigated at temperatures ranging from 623 to 948 K. At temperatures 623, 673 and 723 K the creep is associated with a true threshold stress decreasing with increasing temperature more strongly than the shear modulus of the composite matrix. The true activation energy of creep is close to the activation enthalpy of lattice diffusion in the composite matrix and the true stress exponent of minimum creep strain rate is close to 5. The creep is interpreted in terms of athermal detachment of dislocations from incoherent $Al_{12}(Fe,V)_3Si$ phase particles in the matrix.

At temperatures 773, 798 and 823 K the true threshold stress is not observed. The true stress exponent of minimum creep strain rate increases with increasing stress and the true activation energy of creep is higher than the activation enthalpy of lattice diffusion in the matrix. The creep is interpreted in terms of thermally activated detachment of dislocations from the incoherent $Al_{12}(Fe,V)_3Si$ phase particles.

At temperatures ranging from 873 to 948 K the true threshold stress reappears. However, its origin is different from that at temperatures 623–723 K. The true activation energy is close to the activation enthalpy of grain boundary diffusion and the true stress exponent of minimum creep strain rate is close to 2.5. The creep at these temperatures is interpreted in terms of superplastic flow.

K e y w o r d s: Al-8.5Fe-1.3V-1.7Si-15SiC$_p$ composite, creep, superplastic flow, true threshold stress, strain rate controlling process

[1] Institute of Physics of Materials, Academy of Sciences of the Czech Republic, Žižkova 22, 616 62 Brno, Czech Republic

[2] Department of Mechanical Engineering and Intelligent Systems, The University of Electro-Communications, Chofu, Tokyo, 182-8585 Japan; present address: Institute of Industrial Science, The University of Tokyo, Komaba, Tokyo, 153-8904 Japan

* corresponding author

SPEKTRUM DEFORMAČNÍCH MECHANISMŮ ŘÍDÍCÍCH RYCHLOST CREEPU KOMPOZITU Al-8,5Fe-1,3V-1,7Si-15SiC$_p$ V INTERVALU TEPLOT 623–948 K

Creep slitiny Al-8,5Fe-1,3V-1,7Si vyztužené partikulemi karbidu křemíku – kompozitu Al-8,5Fe-1,3V-1,7Si-15SiC$_p$, je studován při deseti teplotách v intervalu 623–948 K. Při teplotách 623, 673 a 723 K se creep vyznačuje skutečným prahovým napětím klesajícím se vzrůstající teplotou rychleji nežli smykový modul matrice kompozitu. Skutečná aktivační energie creepu je blízká aktivační entalpii mřížkové difuze v matrici kompozitu a skutečný napěťový exponent minimální rychlosti creepu je blízký pěti. Creep je interpretován atermickým odpoutáváním dislokací od nekoherentních částic fáze $Al_{12}(Fe,V)_3Si$ v matrici.

Při teplotách 773, 798 a 823 K není skutečné prahové napětí pozorováno. Skutečný napěťový exponent minimální rychlosti creepu vzrůstá se vzrůstajícím napětím a skutečná aktivační energie creepu je vyšší nežli aktivační entalpie mřížkové difuze v matrici kompozitu. Creep je interpretován jako proces řízený tepelně aktivovaným odpoutáváním dislokací od nekoherentních částic fáze $Al_{12}(Fe,V)_3Si$.

Při teplotách v rozmezí 873–948 K je znovu zaznamenáno skutečné prahové napětí. Jeho původ je však odlišný od původu prahového napětí pozorovaného při teplotách 623–723 K. Skutečná aktivační energie creepu je blízká aktivační entalpii difuze po hranicích zrn a skutečný napěťový exponent minimální rychlosti creepu je blízký 2,5. Creep při těchto teplotách je interpretován superplasticitou.

1. Introduction

An Al-8.5Fe-1.3V-1.7Si (the 8009Al type, numbers indicate wt. %) alloy processed by rapid solidification and powder metallurgy route exhibits remarkable creep resistance up to temperatures around 700 K [1–6]. This creep resistance is due to high volume fraction ($f \cong 0.27$) of fine incoherent particles of the intermetallic $Al_{12}(Fe,V)_3Si$ phase and low coarsening rate of these particles at high temperatures. For the Al-8.5Fe-1.3V-1.7Si alloy the true threshold stress is characteristic [6].

It is well known that the Young's modulus of an aluminium alloy can be increased significantly by discontinuous reinforcement with hard unshearable ceramic particulates, short fibres or whiskers even at temperatures as high as 700 K [7]. This fact motivated Peng et al. [8] and Zhu et al. [9] to reinforce the above alloy with silicon carbide and/or silicon nitride whiskers. Beside increasing the Young's modulus, the discontinuous reinforcement can be expected to introduce the load transfer effect (e.g. refs. [10–12]) that enhances the creep strength, although relatively slightly. As to the Al-8.5Fe-1.3V-1.7Si-15SiC$_p$ composite investigated in the works of the present authors, a far more important effect on the creep strength follows from the fact that as a result of composite processing by powder metallurgy

(see Section 2), fine alumina particles appear in the composite matrix [13].

It should be reminded that, generally, the creep strength of the composite is controlled by creep strength of the composite matrix [13–16], though also the already mentioned load transfer can play a role. Peng et al. [3] have shown that the true threshold stress in creep of an Al-8.5Fe-1.3V-1.7Si alloy reinforced with silicon carbide whiskers (the volume fraction $f_w \sim 0.15$) is significantly higher than the true threshold stress in the unreinforced alloy. This can be explained by the above effect of fine alumina particles present in the composite matrix but not in the matrix alloy.

In one of the previous papers [6], the creep behaviour of an Al-8.5Fe-1.3V-1.7Si alloy (processed by rapid solidification and powder metallurgy) was investigated at three temperatures ranging from 623 to 723 K. The measured minimum creep strain rates covered seven orders of magnitude, the lowest of them were well below 10^{-9} s^{-1}. The creep behaviour was found to be associated with a true threshold stress. The threshold stress was interpreted in terms of the athermal detachment of dislocations from fine incoherent $Al_{12}(Fe,V)_3Si$ phase particles. To account for the temperature dependence of the threshold stress much stronger than that of the shear modulus, the relaxation factor k_R, characterising the strength of the attractive dislocation/particle interaction [17, 18] was assumed to increase with increasing temperature.

Later, the creep behaviour of this alloy, reinforced with 15 vol. % SiC particulates – the Al-8.5Fe-1.3V-1.7Si-15SiC_p composite – was investigated in three temperature regions, namely ranging from 623 to 723 K, from 773 to 823 K and from 873 to 948 K. In the present paper the results of this investigation are reported and analysed.

2. Material and experimental procedures

The fabrication of the Al-8.5Fe-1.3V-1.7Si (Al-8009 type) alloy reinforced with silicon carbide particulates – an Al-8.5Fe-1.3V-1.7Si-15SiC_p composite – was described elsewhere [19]. Briefly, the Al-8.5Fe-1.3V-1.7Si alloy processed by rapid solidification and powder metallurgy [19] was milled and the powder was mixed with nominally 15 vol. % powder of silicon carbide particulates; the nominal mean diameter of silicon carbide particulates was 4.5 μm. The mixed powders were hot consolidated and hot extruded to a rod 12 mm in diameter. From the above treatment the mean grain size less than 1 μm resulted.

The structure of as extruded composite was found sufficiently homogeneous. The composite matrix contained the $Al_{12}(Fe,V)_3Si$ phase particles ($f \cong 0.27$). Also, the matrix of the composite contained a small volume fraction of fine alumina particles appearing during fabrication of the composite by powder metallurgy route. Detailed studies of the structure of similar composites in the prior-to-creep as well as in the post-creep conditions were performed and published by Peng et al. [8].

From the composite rod, specimens for creep tests 4 mm in diameter and 25 mm in gauge length were machined. The constant tensile creep tests were performed in purified argon at three temperature regions, namely 623–723 K, 773–823 K and 873–948 K. The testing temperatures were controlled to within 1 K. The creep elongation was measured by means of linear variable differential transformers coupled with a digital data acquisition system.

Since the testing at the temperatures 873 to 948 K were aimed at superplastic flow under creep-testing conditions, the applied stresses for the creep tests at any given temperature were chosen so as to the minimum creep strain rates cover three orders of magnitude and the lowest minimum creep strain rate be close to 10^{-5} s^{-1}.

All the creep tests were run into tertiary stage and interrupted. No steady state was observed, only minimum creep strain rates $\dot{\varepsilon}_m$ could be defined (cf. ref. [19]).

3. Results and analysis

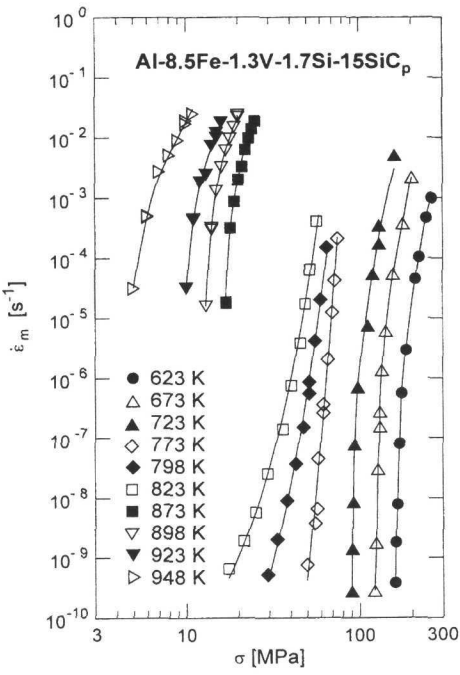

Fig. 1. Relations between minimum creep strain rates $\dot{\varepsilon}_m$ and applied stresses for temperature intervals 623–723 K, 773–823 K and 873 to 948 K.

The minimum creep strain rates $\dot{\varepsilon}_m$ measured at ten temperatures ranging from 623 to 948 K are plotted against applied stresses σ in double-logarithmic co-ordinates in Fig. 1. It can be seen that the relations between $\dot{\varepsilon}_m$ and σ are distinctly separated into three groups. At temperatures 623–723 K the apparent stress exponent of minimum creep strain rate $m_c = (\partial \ln \dot{\varepsilon}_m / \partial \ln \sigma)_T$ (T is the temperature) increases with decreasing stress which clearly indicates the true threshold creep behaviour. The measured minimum creep strain rates cover seven orders of magnitude.

On the contrary, at temperatures 773–823 K the apparent stress exponent m_c *decreases* with decreasing applied stress. Evidently, the true threshold stress is absent at these temperatures. The measured minimum creep strain rates cover six orders of magnitude.

Finally, the $\dot{\varepsilon}_m$ vs. σ relations for temperatures 873–948 K again indicate

the true threshold creep behaviour. In fact, the apparent stress exponent increases with decreasing stress. As it will be shown later, in the temperature interval 873–948 K the superplastic flow takes place. This is why the minimum creep strain rates were only measured for applied stresses, at which they are not lower than 10^{-5} s^{-1}.

In the following, the $\dot{\varepsilon}_m(T, \sigma)$ creep data shown in Fig. 1 will be analysed separately for temperature intervals 623–723 K, 773–823 K and 873–948 K.

3.1 Temperature interval 623–723 K

Relations between the apparent stress exponent m_c and applied stress σ for the temperatures under consideration are shown in Fig. 2. The values of m_c obtained as the derivatives of the $\dot{\varepsilon}_m(T, \sigma)$ relations are indicated by symbols and the apparent stress exponent is denoted as m_c^{exp}, while m_c^{calc} (full curves) were obtained applying the creep equation which will be given later.

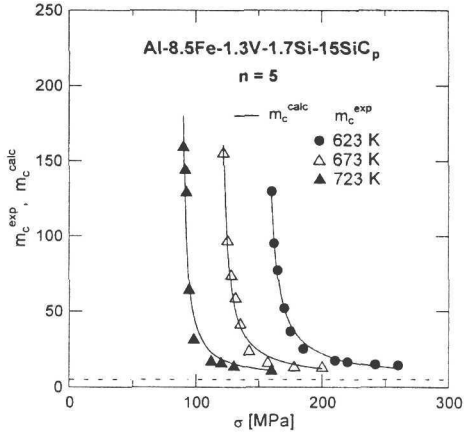

Fig. 2. Temperature interval 623–723 K. Relations between apparent stress exponent m_c and applied stress σ.

Values of the true threshold stress σ_{TH} were determined using the linear extrapolation technique, accepting the value of the true stress exponent n equal to 5 [19]. In Fig. 3 the values of $\dot{\varepsilon}_m^{1/5}$ are plotted against applied stress in double linear co-ordinates. It must be emphasized that for $n = 5$ only the relations between $\dot{\varepsilon}_m^{1/n}$ and σ are linear. The values of σ_{TH} obtained extrapolating $\dot{\varepsilon}_m^{1/5}$ vs. σ relations to $\dot{\varepsilon}_m = 0$ [19] are shown in the figure together with the values of correlation coefficient R_c. Evidently, the threshold stress depends strongly on temperature. The relation between the threshold stress σ_{TH} and temperature is shown in Fig. 4 together with the relation between σ_{TH}/G ratio and temperature; G is the shear modulus of aluminium [20]. The threshold stress decreases with increasing temperature more strongly than the shear modulus G.

Considering the above results as well as some other reported results [21, 22], it is justified to plot $\dot{\varepsilon}_m b^2/D_L$ vs. $(\sigma - \sigma_{TH})/G$ assuming the minimum creep strain rate to be matrix lattice diffusion controlled and accepting the true stress exponent $n = 5$; D_L is the coefficient of lattice self-diffusion in aluminium [23] and b is the length of the Burgers vector in aluminium. Such a plot is shown in Fig. 5. The plotted data points fit a single straight line. This justifies the assumption of the lattice diffusion in the matrix as the minimum creep strain rate controlling process,

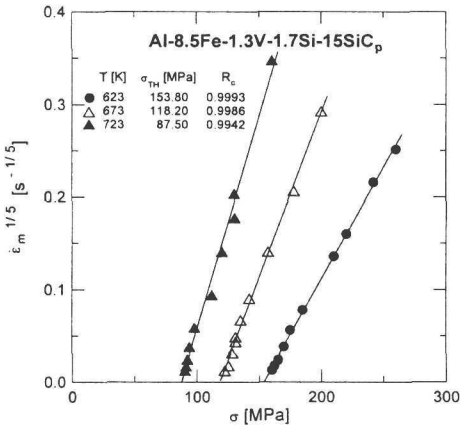

Fig. 3. Temperature interval 623–723 K. Values of $\dot{\varepsilon}_m^{1/5}$ plotted against applied stress in double linear coordinates.

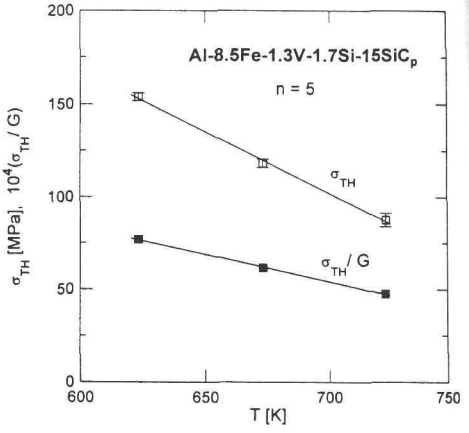

Fig. 4. Temperature interval 623–723 K. Relation between true threshold stress σ_{TH} and σ_{TH}/G ratio and temperature.

as well as the assumption of n close to 5. Thus, the minimum creep strain rate as a function of temperature and applied stress can be expressed as (see e.g. refs. [21, 22])

$$\frac{\dot{\varepsilon}_m b^2}{D_L} = A\left(\frac{\sigma - \sigma_{TH}}{G}\right)^n, \quad n = 5, \tag{1}$$

where A is a dimensionless constant. Combining the creep equation (1) with the definition equation of the apparent activation energy of creep, $Q_c = [\partial \ln \dot{\varepsilon}_m / \partial(-1/RT)]_\sigma$ (R is the gas constant) on one side and with the definition equation of the apparent stress exponent $m_c = (\partial \ln \dot{\varepsilon} / \partial \ln \sigma)_T$ on the other one, the following expressions for the apparent activation energy Q_c and the apparent stress exponent m_c are obtained

$$Q_c = \Delta H_L - \frac{nRT^2}{G}\left(\frac{G}{\sigma - \sigma_{TH}} + \frac{d\sigma_{TH}}{dT} + \frac{n-1}{n}\frac{dG}{dT}\right) \tag{2}$$

and

$$m_c = \frac{n\sigma}{\sigma - \sigma_{TH}}. \tag{3}$$

In Eq. (2) ΔH_L is the activation enthalpy of lattice self-diffusion in aluminium ($\Delta H_L = 142\ \mathrm{kJ \cdot mol^{-1}}$ [23]). From Eqs. (2) and (3) it follows that both m_c and Q_c

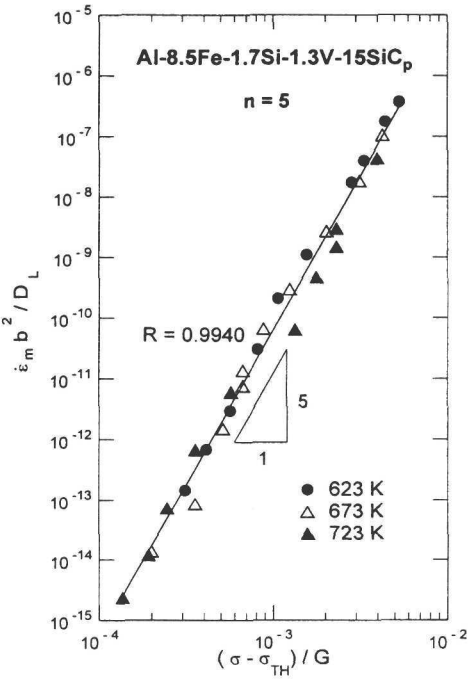

Fig. 5. Temperature interval 623–723 K. Normalized creep strain rates $\dot{\varepsilon}_{\mathrm{m}} b^2/D_{\mathrm{L}}$ plotted against normalized effective stresses $(\sigma - \sigma_{\mathrm{TH}})/G$.

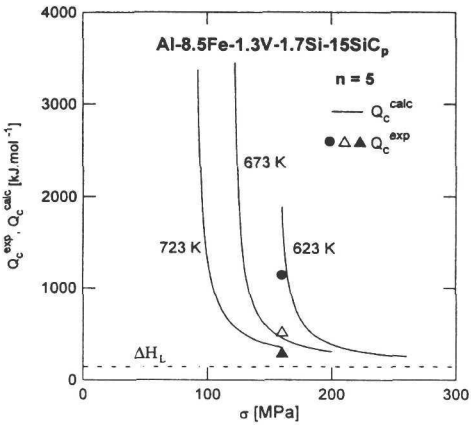

Fig. 6. Temperature interval 623–723 K. Relations between the apparent activation energy $Q_{\mathrm{c}} = Q_{\mathrm{c}}^{\mathrm{calc}}$ and applied stress σ (full curves). The values of $Q_{\mathrm{c}} = Q_{\mathrm{c}}^{\mathrm{exp}}$ for $\sigma = 160$ MPa determined from temperature dependence of $\dot{\varepsilon}_{\mathrm{m}}$ are shown for comparison.

should depend on both the applied stress and temperature, since σ_{TH}/G depends on temperature.

The apparent stress exponent m_{c} will be considered first. The relations between $m_{\mathrm{c}} = m_{\mathrm{c}}^{\mathrm{calc}}$ and applied stress calculated by means of Eq. (3) are shown in Fig. 2 (full curves). It can be seen that $m_{\mathrm{c}}^{\mathrm{calc}}$ are in excellent agreement with the values of $m_{\mathrm{c}}^{\mathrm{exp}}$ obtained as the derivatives of experimental $\dot{\varepsilon}_{\mathrm{m}}(T, \sigma)$ relations (symbols), Fig. 1. This strongly supports the validity of the creep equation (1).

The relations between the apparent activation energy $Q_{\mathrm{c}} = Q_{\mathrm{c}}^{\mathrm{calc}}$ calculated by means of Eq. (2) and applied stress are shown in Fig. 6. Because of very strong temperature and applied stress dependence of the minimum creep strain rates, the $Q_{\mathrm{c}} = Q_{\mathrm{c}}^{\mathrm{exp}}$ can be estimated in a conventional way from the temperature

dependence of $\dot{\varepsilon}_m(T,\sigma)$ creep data for one applied stress only, namely for $\sigma =$ $= 160$ MPa. However, it should be emphasized that the calculated values of $Q_c =$ $= Q_c^{calc}$ were shown [21] to be in very good agreement with the values of $Q_c =$ $= Q_c^{exp}$ determined from the temperature dependence of $\dot{\varepsilon}_m(\sigma)$. For the composite investigated in the present work the values of Q_c^{exp} at $\sigma = 160$ MPa are plotted in Fig. 6. The agreement of Q_c^{calc} with Q_c^{exp} is quite good, which again supports the correctness of the creep equation (1).

Note that the apparent stress exponent m_c reaches very high values at applied stresses only slightly higher than the threshold stress at each temperature (Fig. 2). At the *highest* applied stresses this exponent is still higher than the true stress exponent $n = 5$. The apparent stress exponent decreases with increasing temperature.

Similarly, also the apparent activation energy Q_c reaches extremely high value at applied stresses slightly higher than the threshold stresses (Fig. 6). At each applied stress, the apparent activation energy decreases with increasing temperature. At the highest applied stresses considered, the apparent activation energy Q_c is still higher than the activation enthalpy of the lattice diffusion in the composite matrix.

It was shown [19] that the load transfer effect does not play any significant role in creep strengthening of the composite investigated. The load transfer contribution to the creep behaviour of the investigated composite will be discussed in some detail in Section 4.

The true threshold creep behaviour of the composite at temperatures 623–723 K is associated with the presence of fine incoherent $Al_{12}(Fe,V)_3Si$ phase particles as well as the presence of a small volume fraction of alumina particles (appearing during PM processing) in the composite matrix. Both these types of particles are incoherent with the matrix. Hence, they are expected to attract the mobile dislocations under creep conditions [17, 18]. Then, the controlling step of climb of a dislocation past a particle is represented by detachment of the dislocation from departure side of the particle after the climb process over it had been finished. The stress needed to detach a dislocation from an interacting particle – the detachment stress σ_d expressed as [17]

$$\sigma_d = \sigma_{OB}\sqrt{1 - k_R^2} \tag{4}$$

is then identified with the true threshold stress [18]. In Eq. (4), σ_{OB} is the Orowan bowing stress and k_R is the relaxation factor characterising the strength of the attractive dislocation/particle interaction. The Orowan bowing stress can be expressed by a simple formula [24]

$$\sigma_{OB} = \frac{0.84\ MGb}{\lambda - d}, \tag{5}$$

in which M is the Taylor factor, λ is the mean interparticle spacing and d is the mean particle diameter. The Orowan bowing stress is thus proportional to the shear modulus G and, consequently, the σ_{OB}/G ratio does not depend on temperature. The experimentally determined true threshold stress σ_{TH} depends on temperature more strongly than the shear modulus G of the matrix. Therefore, σ_{TH} cannot be identified with the detachment stress σ_d unless a temperature dependence of the relaxation factor k_R is admitted. At the present time, the relaxation factor cannot be calculated from the first principles. Arzt and Wilkinson [17] modelled the attractive dislocation/particle interaction in a simple way in terms of dislocation line energies Γ and Γ' in the matrix and in the particle/matrix interface, respectively. Accepting the model of these authors and taking into account possible role of impurities (decreasing the energy Γ') and forming atmospheres at the departure sides of interacting particles [13], it has been shown [25, 26] that a temperature dependence of the relaxation factor can be realistically expected.

An idea on possible values of k_R and, especially, on its temperature dependence, can be obtained analysing proper $\dot{\varepsilon}_m(T, \sigma)$ creep data. To get such an idea for the composite investigated in the present work, Eq. (4) is written in the form (cf. ref. [17, 18])

$$\frac{\sigma_d}{G} = C_0\sqrt{1 - k_R^2}, \tag{6}$$

where $C_0 = \sigma_{OB}/G$ is a temperature independent constant equal to $0.84\, Mb/(\lambda - d)$, since $\sigma_{OB} \propto G$. Thus, the constant C_0 can be calculated from structure data such as λ and d. However, because of uncertainty of λ and d, it is preferred to assume a value of k_R for one temperature, namely 673 K, equal to 0.85 (see refs. [13, 14]) and setting $\sigma_d/G = \sigma_{TH}/G = 6.15 \times 10^{-3}$ for this temperature, the constant $C_0 = \sigma_{TH}/G\sqrt{1 - k_R^2}$ is obtained equal to 1.17×10^{-2}. Accepting this value of C_0, values of k_R equal to 0.75 and 0.91 are obtained for 623 and 723 K, respectively. These values of k_R seem reasonable. It should be pointed out that the factor k_R apparently approaches a constant "critical" value of 0.94 with the temperature approaching 800 K, Fig. 7. This "critical" value of k_R followed from the analyses of Arzt and Wilkinson [17] and Arzt and Rösler [18].

The above assumption on temperature dependence of the relaxation factor k_R seems to be, at the present time at least, the only, although still a some-

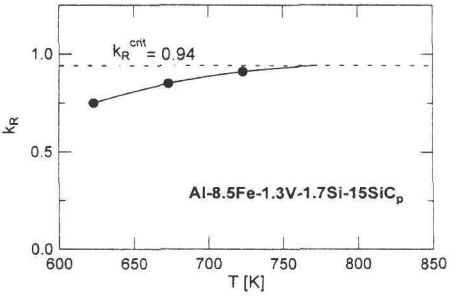

Fig. 7. Temperature interval 623–723 K. Temperature dependence of the relaxation factor k_R.

what speculative, explanation of the temperature dependence of the normalized true threshold stress σ_{TH}/G as obtained analysing the experimental $\dot{\varepsilon}_m(T, \sigma)$ creep data for discontinuous dispersion strengthened aluminium matrix composites.

3.2 Temperature interval 773–823 K

At temperatures ranging from 773 to 823 K the true threshold stress is not observed. In fact, the apparent stress exponent of the minimum creep strain rate decreases with decreasing applied stress in this temperature interval (Fig. 1). The absence of the true threshold stress at temperature interval 773–823 K can be interpreted in terms of a transition from athermal to thermally activated detachment of dislocations from incoherent particles in the composite matrix [27–29]. The thermally activated detachment of dislocations from interacting particles was considered by Rösler and Arzt [30] when developing the creep equation of dispersion strengthened alloys. This equation can be written as

$$\frac{\dot{\varepsilon}_m b^2}{D_L} = C \exp\left(-\frac{G b^2 d_p [(1 - k_R)(1 - \sigma/\sigma_d)]^{3/2}}{2kT}\right), \tag{7}$$

where

$$C = 6\lambda\rho b \tag{8}$$

is the structure factor. In Eq. (7) d_p is the particle diameter, in Eq. (8) ρ is the density of mobile dislocations. According to Eq. (7) the true activation energy (activation enthalpy) of creep is higher than the activation enthalpy of lattice diffusion in the composite matrix. The true activation energy of creep $\Delta H_c > \Delta H_L$ is indicated in Fig. 8. In fact, the $\dot{\varepsilon}_m b^2/D_L$ plotted against σ/G for the temperatures under consideration do not fit a single curve.

The values of σ_d and k_R can be calculated for various applied stresses and temperatures using the procedure proposed by Rösler and Arzt [30]. In the following, a slightly different procedure to correlate the $\dot{\varepsilon}_m(T, \sigma)$ creep data with the Rösler–Arzt model creep equation is used. The modification of the fitting procedure is based on the assumption (see Section 3.1) following from the hypothesis that to identify the detachment stress σ_d in Eq. (6) with the threshold stress obtained analysing the experimental $\dot{\varepsilon}_m(T, \sigma)$ creep data, the increase of the relaxation factor k_R with temperature must be admitted. The "critical" value of k_R is close to 0.94 above 750 K (Fig. 7). Accepting this fixed value of k_R, the equation for σ_d can be written as [29]

$$\left(\frac{\sigma}{\sigma_d}\right)^3 - \left(\frac{\sigma}{\sigma_d}\right)^2 = -\frac{K(T)^2}{(1 - k_R)^3}, \tag{9}$$

where $K(T) = 4kTm_c/3Gb^2d_p$. The values of the detachment stress σ_d calculated for the temperatures under consideration accepting $k_R = 0.94$ are listed in Table 1 for an applied stress $\sigma = 50$ MPa. Using these results, the experimental $\dot{\varepsilon}_m(T,\sigma)$ creep data in $\dot{\varepsilon}_m b^2/D_L$ vs. σ/G co-ordinates are compared with the creep equation (7) in Fig. 8. The agreement of the $\dot{\varepsilon}_m(T,\sigma)$ creep data with the prediction of Rösler–Arzt model – the creep equation (7) – is very good. However, the value of the structure factor C following from the fitting procedure should be close to that calculated from the structure data (Eq. (8)), before the correlation could be considered fully satisfactory. But the difference between the values of C following from the fitting procedure differ from that calculated from the structure data significantly. This difference was discussed extensively in several papers of the present authors [27, 29, 31] with the conclusion that it has to be considered a deficiency of the Rösler-Arzt model [30] in its present formulation (see also ref. [32]).

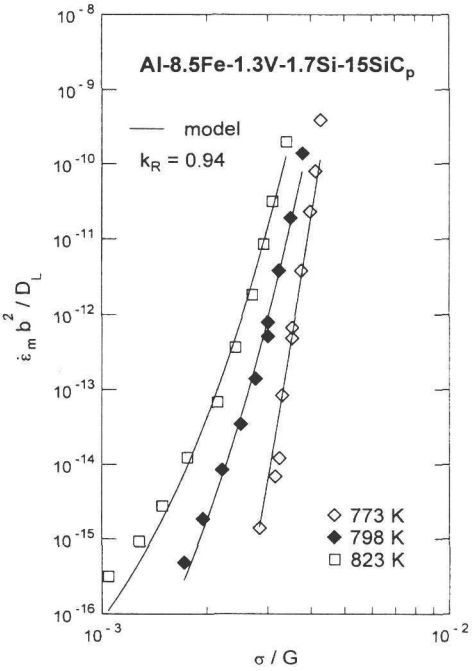

Fig. 8. Temperature interval 773–823 K. The relations between $\dot{\varepsilon}_m b^2/D_L$ and σ/G predicted by the Rösler–Arzt model [30] compared with $\dot{\varepsilon}_m b^2/D_L$ vs. σ/G relation obtained from the experimental $\dot{\varepsilon}_m(T,\sigma)$ creep data.

Recently, Ma and Tjong [33] published results of an extensive investigation of creep in an Al-8.5Fe-1.3V-1.7Si-15SiC$_p$ composite at temperatures 723–823 K. They found that not only at 723 K (as in the present work) but also at 748 K and, especially at 773 and 823 K, the

Table 1. Values of the detachment stress σ_d calculated by means of Eq. (9) for various temperatures and an applied stress $\sigma = 50$ MPa accepting the relaxation factor $k_R = 0.94$. Values of the structure factor C obtained comparing the $\dot{\varepsilon}_m(T,\sigma)$ creep data with the prediction of the Rösler-Arzt model [30]

$T = 773$ K		$T = 798$ K		$T = 823$ K	
σ_d [MPa]	C	σ_d [MPa]	C	σ_d [MPa]	C
102.6	1.17×10^{-7}	169.2	5.93×10^{-1}	166.3	2.57×10^{0}

apparent stress exponent m_c increases with decreasing applied stress, thus indicating the true threshold stress. This is in contradiction with the present results for temperatures 773–823 K, which is difficult to account for in the present report.

It is worth mentioning that the results very similar to those for Al-8.5Fe-1.3V-1.7Si-15SiC$_p$ composite Ma and Tjong [33] reported also for unreinforced Al-8.5Fe-1.3V-1.7Si alloy (see later Fig. 14).

3.3 Temperature interval 873–948 K

The minimum creep strain rates measured at temperatures 873, 898, 923 and 948 K are plotted against applied stresses in Fig. 1. It can be seen that the apparent stress exponent m_c increases with decreasing applied stress at each temperature, which again indicates a true threshold creep behaviour.

In Figs. 9a,b values of $\dot{\varepsilon}_m^{1/n}$ are plotted against applied stress for $n = 2$ and $n = 2.5$, respectively. Only these values of the true stress exponent n provide the linear relations between $\dot{\varepsilon}_m^{1/n}$ and σ in double linear co-ordinates. Inspecting the values of the correlation coefficient R_c given in Fig. 9, in which also the values of the true threshold stress σ_{TH} are presented, one should prefer $n = 2.5$ to $n = 2$. Beside, for $n = 2$ the true threshold stress is higher than the lowest applied stress. This implies a negative effective stress $\sigma_e = \sigma - \sigma_{TH}$, which is absurd. (In the present paper, the true threshold stress is generally denoted σ_{TH} regardless of its

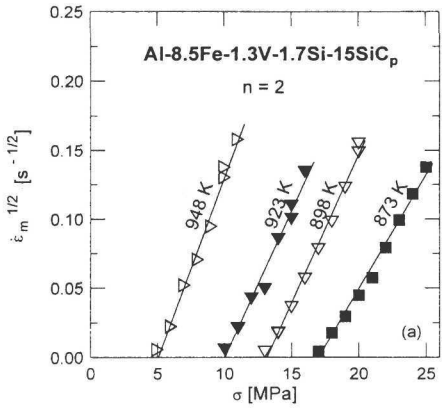

T [K]	σ_{TH} [MPa]	R_c
873	17.01	0.9951
898	13.18	0.9962
923	10.02	0.9896
948	5.07	0.9950

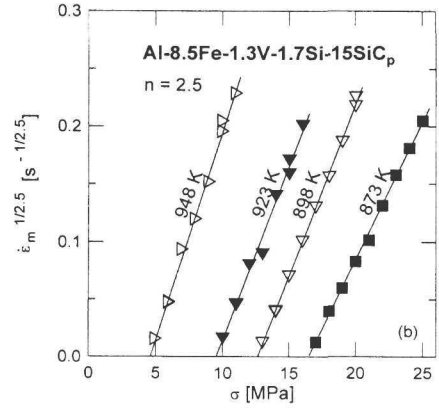

T [K]	σ_{TH} [MPa]	R_c
873	16.47	0.9993
898	12.65	0.9994
923	9.53	0.9942
948	4.61	0.9976

Fig. 9. Temperature interval 873–948 K. Values of $\dot{\varepsilon}_m^{1/n}$ plotted against applied stress σ for $n = 2$ (a) and $n = 2.5$ (b).

origin, which is certainly different in the interval 623–723 K and the interval 873–948 K).

The values of σ_{TH} obtained accepting $n = 2.5$ are plotted against temperature in Fig. 10, in which also the σ_{TH}/G ratios are plotted against temperature. It can be seen that both σ_{TH} and σ_{TH}/G decrease with increasing temperature.

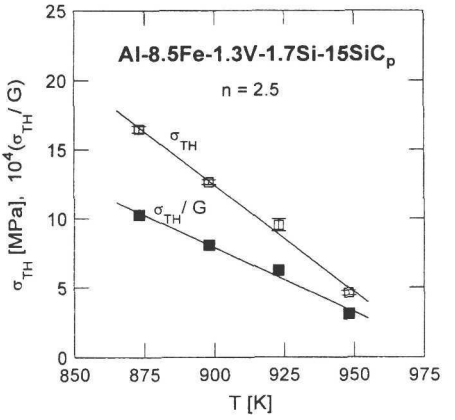

Fig. 10. Temperature interval 873–948 K. Values of the true threshold stress σ_{TH} plotted against temperature. The relation between σ_{TH}/G and T are also shown in the figure.

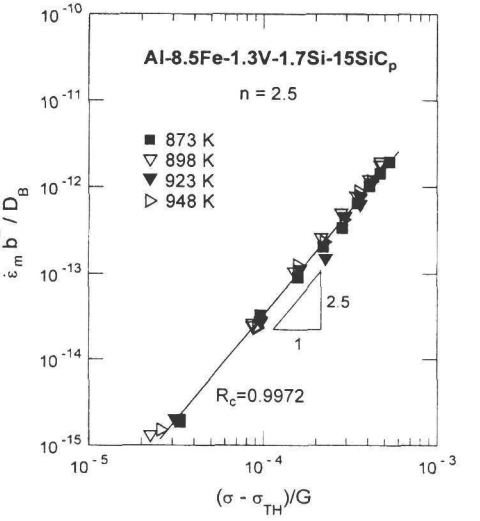

Fig. 11. Temperature interval 873–948 K. Normalized minimum creep strain rates $\dot{\varepsilon}_m b^2/D_B$ plotted against normalized effective stresses $(\sigma - \sigma_{TH})/G$.

In Fig. 11, the normalized minimum creep strain rates $\dot{\varepsilon}_m b^2/D_B$ are plotted against normalized effective stress $(\sigma - \sigma_{TH})/G$; $D_B = 1.7 \times 10^{-5} \exp[-72.4/RT]$ $(m^2 \cdot s^{-1})$ is the coefficient of grain boundary diffusion in aluminium [34, 35]. All the data points can be fitted by a single straight line in these co-ordinates, the slope of the line is approximately equal to the true stress exponent n, i.e. to 2.5. This result strongly suggests that under the external conditions given, the normalized minimum creep strain rate of the composite investigated is controlled by grain boundary diffusion and the true stress exponent of this strain rate is close to, but not higher, than 2.5. Thus the $\dot{\varepsilon}_m b^2/D_B$ vs. $(\sigma - \sigma_{TH})/G$ relation strongly suggests the superplastic flow and, thus, it can be described by the equation (e. g. refs.

[36–39])

$$\frac{\dot{\varepsilon}_{\mathrm{m}} b^2}{D_{\mathrm{B}}} = A_{\mathrm{S}} \left(\frac{b}{d}\right)^p \left(\frac{\sigma - \sigma_{\mathrm{TH}}}{G}\right)^n , \tag{10}$$

where d is the mean grain diameter, p is the exponent of the inverse mean grain diameter and A_{S} is the dimensionless constant. Usually, p is equal to 2 [38, 39] and also n is usually found close to 2 [38, 39], although Kim et al. [37] found $n = 2.5$ for Al-2124Al-20SiC$_{\mathrm{p}}$ composite. The apparent activation energy Q_{c} is in the following relation to the activation enthalpy of grain boundary diffusion ΔH_{B}(cf. Eq. (2)):

$$Q_{\mathrm{c}} = \Delta H_{\mathrm{B}} - \frac{nRT^2}{G} \left(\frac{G}{\sigma - \sigma_{\mathrm{TH}}} \frac{\mathrm{d}\sigma_{\mathrm{TH}}}{\mathrm{d}T} + \frac{n-1}{n} \frac{\mathrm{d}G}{\mathrm{d}T}\right). \tag{11}$$

The apparent stress exponent m_{c} is in the relation to the true stress exponent n expressed by Eq. (3).

Equation (11) makes it possible to calculate the apparent activation energy Q_{c} as a function of applied stress at each temperature, since n and $\sigma_{\mathrm{TH}} = \sigma_{\mathrm{TH}}(T)$ are known from experiment. The calculated relations between Q_{c} and σ are shown in Fig. 12a. It can be seen that the apparent activation energy Q_{c} decreases strongly with increasing applied stress at each testing temperature and with increasing temperature at any applied stress. At applied stresses only slightly higher than the respective threshold stress, the calculated values of Q_{c} are extremely high. The values of Q_{c} corresponding to low applied stresses are not included in Fig. 12a, because of a practical reason; in fact, e.g. at the temperature 898 K and 13 MPa, the calculated value of Q_{c} amounts to 7500 kJ·mol^{-1}, and thus it is two orders of magnitude higher than the activation enthalpy of grain boundary diffusion. Note (Fig. 12a) that even at the highest applied stresses the values of Q_{c} are much higher than the activation enthalpy of grain boundary diffusion $\Delta H_{\mathrm{B}} = 72.4$ kJ·mol^{-1} [34, 35].

Quite a natural requirement is to compare calculated values of Q_{c} with those obtained from the experimental $\dot{\varepsilon}_{\mathrm{m}}(T, \sigma)$ data by the conventional method, i.e. from the $\ln \dot{\varepsilon}_{\mathrm{m}}$ vs. $1/T$ relations for various applied stresses. However, such a comparison can be performed in a very limited extent because of the very strong temperature and applied stress dependence of the minimum creep strain rate (Fig. 1). In fact, the $\dot{\varepsilon}_{\mathrm{m}}(T, \sigma)$ data in this figure make it possible to obtain only one $\ln \dot{\varepsilon}_{\mathrm{m}}$ vs. $1/T$ relation, namely for $\sigma = 17$ MPa. Values of Q_{c} for 873, 898 and 923 K obtained from this relation are plotted in Fig. 12a. The $Q_{\mathrm{c}}(T)$ data points, plotted in this figure, fit the respective curves calculated by means of Eq. (11) satisfactorily.

The extremely high and strongly applied stress and temperature dependent values of the apparent activation energy Q_{c} are associated with the true threshold stress σ_{TH} decreasing with increasing temperature (Fig. 10). In fact, if the threshold

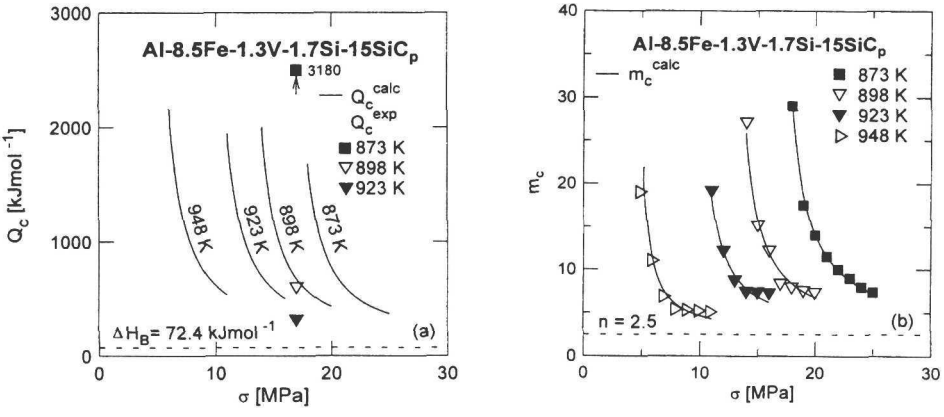

Fig. 12. Temperature interval 873–948 K. (a) Calculated relations between apparent activation energy $Q_c \equiv Q_c^{calc}$ and applied stress σ (full curves). Values of $Q_c \equiv Q_c^{exp}$ obtained from the experimental $\ln \dot{\varepsilon}_m$ vs. $1/T$ relation for 17 MPa are shown for comparison. (b) Calculated relations between apparent stress exponent $m_c \equiv m_c^{calc}$ and applied stress (full curves). Values of $m_c \equiv m_c^{exp}$ obtained from $\ln \dot{\varepsilon}_m$ vs. $\ln \sigma$ relations (Fig. 1) are shown for comparison (data point symbols).

stress were temperature independent ($d\sigma_{TH}/dT$ were zero), Eq. (11) would be reduced to the well known equation (e.g. ref. [40])

$$Q_c = \Delta H_B - (n-1)\frac{RT^2}{G}\frac{dG}{dT}. \tag{12}$$

Consequently, Q_c would be stress independent and would increase with temperature from 81.9 kJ·mol^{-1} at 873 K to 84.5 kJ·mol^{-1} at 948 K. Thus, the first term in the brackets in Eq. (11) is evidently responsible not only for the strong temperature but also for the strong applied stress dependence of Q_c.

Relations between the apparent stress exponent m_c and applied stress for the temperatures ranging from 873 to 948 K calculated by means of Eq. (3) are shown by full curves in Fig. 12b. The calculated apparent stress exponent decreases very strongly with increasing applied stress, and at any given applied stress it decreases with increasing temperature. Again, the values of m_c corresponding to the lowest stresses under consideration are not presented in this figure, because they are very high compared with the value of the true stress exponent n. In fact, at the temperature 898 K and $\sigma = 13$ MPa, m_c is as high as 92.8. At the highest applied stresses the values of m_c are still significantly higher than 2.5, thus e.g. at 898 K and 20 MPa, $m_c = 6.8$.

From the experimental $\dot{\varepsilon}_m(T, \sigma)$ relations, values of $m_c(\sigma)$ can be obtained as the derivatives of $\dot{\varepsilon}_m(\sigma)$ relations with respect to σ, Fig. 12b. From this figure it can be seen that the data points obtained this way fit the $m_c(\sigma)$ curves calculated by means of Eq. (3) excellently, which, of course, strongly supports the correctness of Eq. (10).

The superplastic flow can be described by Eq. (10) with $p = 2$ and $n = 2$ [39]. In the present investigation the true stress exponent $n = 2.5$ is preferred to $n = 2$ (cf. Figs. 9a,b) similarly as in the work of Kim et al. [37]. Superplastic flow is considered (cf. refs. [36, 38, 39]) to be due to grain boundary sliding accommodated with glide of lattice dislocations in zones along grain boundaries. The grain boundary sliding (GBS) is assumed to occur by motion of grain boundary dislocations in the grain boundary planes [40]. The Burgers vector of a grain boundary dislocation generally differs from that of the lattice dislocation and does not generally lie in the grain boundary plane. Consequently, a grain boundary dislocation (which cannot leave the boundary to enter the lattice) moves in the grain boundary by a combination of conservative and non-conservative modes and, thus, its motion is generally grain boundary diffusion controlled [40].

In the Al-8.5Fe-1.3V-1.7Si-15SiC_p composite, particulates or particles of at least three phases are embedded in the matrix solid solution: (i) relatively coarse silicon carbide particulates (SiC_p); (ii) relatively fine $Al_{12}(Fe,V)_3Si$ phase particles and (iii) fine alumina particles appearing in the PM processing of the composite. Of course, some of these particulates and particles are located in grain boundaries and represent obstacles to motion of grain boundary dislocations and/or to grain boundary sliding. Occasionally, some of the grain boundary dislocations can be pushed through the gaps between the neighbouring obstacles, giving rise to a relatively low threshold stress analogous to the Orowan bowing stress. The dislocation loops left around the obstacles must disappear by climb/glide motion in the obstacle/matrix interface. But most of the obstacles (particulates and particles) must be bypassed by *localized* climb/glide motion, since no segment of a moving grain boundary dislocation can enter the matrix lattice. This localized climb/glide motion generates the true threshold stress.

However, although the above speculation on the origin of the true threshold stress seems acceptable and worth of further analysis, it does not provide any idea on the relatively strong temperature dependence of the true threshold stress responsible for very high and strongly applied stress and temperature dependent apparent activation energy Q_c and the apparent stress exponent m_c of the superplastic flow process in the composite.

4. Discussion

4.1 Introduction

At temperatures ranging from 623 to 948 K three strain rate controlling deformation mechanisms acting under creep conditions (i. e. at constant temperature and constant applied stress) were identified. These strain rate controlling mechanisms differ in the true activation energies as well as in the true stress exponents of minimum creep strain rate.

As it is shown in Fig. 1, the strain rate behaviours at temperatures 623–723 K as well as at temperatures 873–948 K are associated with true threshold stresses differing in their origins. In the intermediate interval, i.e. 773–823 K, the true threshold stress is absent. The strain rate behaviour in the above temperature intervals was analysed in detail in Section 3. However, in these analyses the load transfer effect was left aside, although it was mentioned in Sections 1 and 3.1. In the literature, the load transfer effect was considered in connection with the results similar to those presented in Section 3.1 and 3.3, i.e. at external conditions, under which the true threshold behaviour was shown to take place. But the load transfer effect should be as well discussed in connection with the strain rate behaviour in the temperature interval in which the true threshold stress is absent, which seems to be a new phenomenon in the creep behaviour of discontinuous aluminium alloy matrix composites processed by powder metallurgy route.

4.2 Load transfer

Generally, when a discontinuous composite is subjected to external load, this load is partly transferred from the composite matrix to the unshearable reinforcement. Consequently, the stress in the composite matrix is lowered, which results in composite strength increase, since this strength is controlled by that of the matrix. The possibility of such a strengthening in the short fibre composite was first considered by Kelly and Street [41, 42]. Recent experiments have provided a direct evidence of load transfer in a 6061Al alloy reinforced with silicon carbide particulates [25]. See also ref. [14].

4.2.1 *Load transfer in strain rate behaviour associated with the true threshold stress*

Park and Mohamed [25] used the concept of load transfer in an analysis of the creep in a 6061Al alloy reinforced with SiC particulates, exhibiting the true threshold behaviour. These authors introduced an effective stress defined as $(1 - \alpha)(\sigma - \sigma_{TH})$, where α is the load transfer coefficient; values of α range from zero, in the absence of any load transfer, to one, when all the load is transferred. When

the effective stress $(\sigma - \sigma_{TH})$ in the creep equation (1) and Eq. (10), respectively, is replaced by the effective stress defined above, these equations can be written as

$$\frac{\dot{\varepsilon}_m b^2}{D} = A' \left[\frac{(1-\alpha)(\sigma - \sigma_{TH})}{G} \right]^n, \tag{13}$$

where D is the appropriate diffusion coefficient, A' is an appropriate dimensionless constant and n is the appropriate true stress exponent. Combining this equation with the definition equation of the apparent activation energy, $Q_c = [\partial \ln \dot{\varepsilon}_m / \partial(-1/RT)]_\sigma$, the apparent activation energy can be expressed as

$$Q_c = \Delta H - \frac{nRT^2}{G} \left(\frac{\sigma - \sigma_{TH}}{G} \frac{d\sigma_{TH}}{dT} + \frac{n-1}{n} \frac{dG}{dt} \right) - \frac{nRT^2}{1-\alpha} \frac{d\alpha}{dT}. \tag{14}$$

In Eq. (14), ΔH is the activation enthalpy of the proper diffusion process. The coefficient α decreases with increasing temperature but is independent of applied stress.

In the present paper, only the $\dot{\varepsilon}_m(T, \sigma)$ data for temperatures ranging from 873 to 948 K will be considered; at these temperatures, superplastic flow takes place (see Section 3.3). Thus $\Delta H \equiv \Delta H_B$ and $n = 2.5$ at these temperatures. An analysis for the temperature interval 623 to 723 K would be qualitatively similar.

Park and Mohamed [25] proposed a procedure to estimate the load transfer coefficient from experimental $\dot{\varepsilon}_m(T, \sigma)$ creep data. The procedure will be neither outlined here nor applied to calculate the load transfer coefficient as a function of temperature. Instead, referring to Li and Langdon's Table 4 in ref. [43], both α and $d\alpha/dT$ will be chosen arbitrarily but reasonably as 0.5 and -2.5×10^{-3} K^{-1}, respectively. Accepting these values of α and $(d\alpha/dT)$, the contributions $-[nRT^2/(1-\alpha)](d\alpha/dT)$ (load transfer contributions – LTC) equal to 79.3, 83.9, 88.6 and 93.5 $kJ \cdot mol^{-1}$ are obtained for the temperatures 873, 898, 923 and 948 K, respectively.

To estimate the effect of temperature dependence of the load transfer coefficient α on the values of the apparent activation energy Q_c, the testing temperature of 923 K and the applied stresses of 12 and 16 MPa will be considered. At 923 K, LTC equals to 88.6 $kJ \cdot mol^{-1}$ (see above). By means of Eq. (14) the activation energy $Q_c = 1281.2$ $kJ \cdot mol^{-1}$ is obtained for 923 K and 12 MPa, while the contribution of the term $-[nRT^2/(\sigma - \sigma_{TH})](d\sigma_{TH}/dT)$ (threshold stress contribution – TSC) amounts to 1110.6 $kJ \cdot mol^{-1}$. Thus the LTC to Q_c represents only about 6.9 % of Q_c, while TSC represents 86.7 % of Q_c.

At the same temperature but the higher applied stress of 16 MPa, the apparent activation energy $Q_c = 594.6$ $kJ \cdot mol^{-1}$ is obtained by means of Eq. (14). The LTC is again equal to 88.6 $kJ \cdot mol^{-1}$, representing now 14.9 % of Q_c while the TSC is equal to 424 $kJ \cdot mol^{-1}$ and thus represents 71.3 % of Q_c.

The above analysis clearly shows that the high values of the apparent activation energy of superplastic flow in an Al-8.5Fe-1.3V-1.7Si-15SiC$_p$ composite cannot be explained merely by the temperature dependence of load transfer coefficient α (cf. ref. [43]). Instead, it is the temperature dependence of the true threshold stress that affects the value of the apparent activation energy Q_c dominantly.

The role of temperature dependence of the true threshold stress in relation to the values of the apparent activation energy Q_c has been already discussed in Section 3.3, where the load transfer effect has not yet been taken into account. It is interesting to note that replacing $(\sigma - \sigma_{TH})$ in Eq. (3) by $(1 - \alpha)(\sigma - \sigma_{TH})$ the apparent stress exponent twice as high follows from this equation for the accepted value of $\alpha = 0.5$.

The above accepted definition of the effective stress incorporating load transfer coefficient $\sigma_e = (1 - \alpha)(\sigma - \sigma_{TH})$ implies that the load transfer starts to take place only after the threshold stress is surpassed by the applied stress, in other words, that load transfer is associated with some plastic strain. Referring to the recent papers by Li et al. [44] and Shi et al. [12], Li and Langdon [43] prefer to define the effective stress as: $\sigma_e = (1 - \alpha)\sigma - \sigma_{TH}$. Introducing the *apparent* threshold stress $\sigma_{TH}^{app} = \sigma_{TH}/(1 - \alpha)$, the effective stress is expressed as $\sigma_e = (1 - \alpha)(\sigma - \sigma_{TH}^{app})$. Li and Langdon [43] believe that using the linear extrapolation method to estimate the threshold stress, it is just the apparent threshold stress that is obtained. If this is the case, the analysis in terms of the effective stress defined as $\sigma_e = (1 - \alpha)(\sigma - \sigma_{TH}^{app})$ does not *qualitatively* differ as to the $Q_c(T, \sigma)$ from that above in terms of the effective stress $\sigma_e = (1 - \alpha)(\sigma - \sigma_{TH})$.

Frequently, the origin of high values of the apparent activation energy Q_c is left out of consideration and the quantity which is believed to represent the *true* activation energy is determined plotting $\ln \dot{\varepsilon}$ vs. $1/T$ for a constant value of the effective stress $\sigma_e = (\sigma - \sigma_{TH})$ (e. g. ref. [37]). However, such a procedure seems questionable, since the true threshold stress itself depends on temperature.

4.2.2 *Load transfer in creep not associated with the true threshold stress*

In the temperature interval 773–823 K, the true threshold stress is absent (Section 3.2). Using the model developed by Rösler and Arzt [30], the creep behaviour can be interpreted in terms of thermally activated detachment of dislocations from incoherent particles, predominantly the particles of the $Al_{12}(Fe,V)_3Si$ phase. Nevertheless, the load transfer effect must still be expected. To take this effect into account the applied stress σ in Eq. (7) should be replaced by $(1 - \alpha)\sigma$. Unfortunately, no procedure to estimate the load transfer coefficient α and its temperature dependence from the experimental $\dot{\varepsilon}_m(T, \sigma)$ creep data seems to be available at the present time.

However, to get an idea on the load transfer effect under consideration, this effect can be modelled choosing arbitrarily, but reasonably, a value of the coefficient

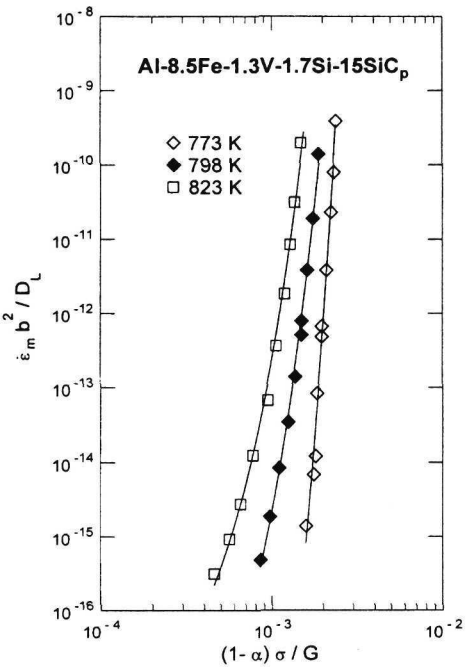

Fig. 13. Temperature interval 773–823 K. Relations between normalized creep strain rates $\dot{\varepsilon}_{\mathrm{m}} b^2/D_{\mathrm{L}}$ and the normalized stresses $(1-\alpha)\sigma/G$; α is the load transfer coefficient.

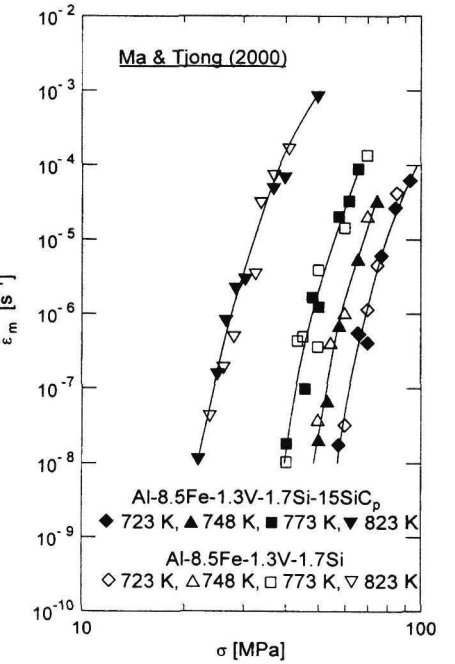

Fig. 14. Relations between $\dot{\varepsilon}_{\mathrm{m}}$ and σ for an Al-8.5Fe-1.3V-1.7Si alloy and Al-8.5Fe-1.3V-1.7Si-15SiC$_{\mathrm{p}}$ composite for temperatures 723–823 K. Data of Ma and Tjong [33].

α equal to 0.5 at 798 K and $\mathrm{d}\alpha/\mathrm{d}T = -2.5 \times 10^{-3}$ K^{-1}. Then α is equal to 0.44 at 773 K and to 0.56 at 823 K. The normalized creep strain rates $\dot{\varepsilon}_{\mathrm{m}} b^2/D_{\mathrm{L}}$ are plotted against the normalized stress $(1-\alpha)\sigma/G$ in Fig. 13. Provided the values of α and $\mathrm{d}\alpha/\mathrm{d}T$ are correctly chosen, the relations in Fig. 13 should represent those for unreinforced Al-8.5Fe-1.3V-1.7Si alloy. Unfortunately, the relations between $\dot{\varepsilon}_{\mathrm{m}} b^2/D_{\mathrm{L}}$ vs. σ/G have not yet been obtained for this alloy; consequently, the comparison is not possible.

In this context, the recently published paper by Ma and Tjong [33] must be mentioned. These authors found that the $\dot{\varepsilon}$ vs. σ relations are apparently identical for the Al-8.5Fe-1.3V-1.7Si alloy and this alloy reinforced with silicon carbide particulates. Both the Al-8.5Fe-1.3V-1.7Si alloy and the Al-8.5Fe-1.3V-1.7Si-15SiC$_{\mathrm{p}}$ composite exhibit true threshold behaviour even at temperatures 723 to 823 K (Fig. 14) in contrast to the present results (Fig. 1). Consequently, the load trans-

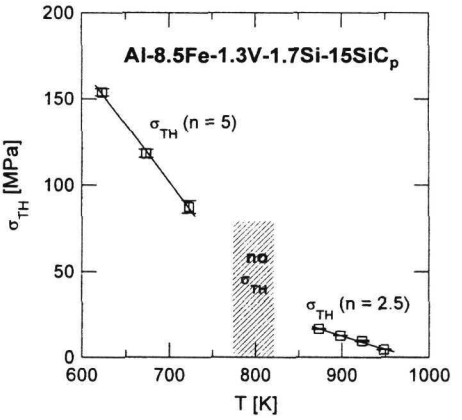

Fig. 15. The true threshold stress behaviour of the composite at temperatures ranging from 623 to 948 K. See Section 3.1 for 623–723 K, where $n = 5$; Section 3.2 for 773–823 K at which no threshold stress is observed and Section 3.3 for 873–948 K, where $n = 2.5$ and the superplastic flow is associated with a true threshold stress.

fer coefficient $\alpha = 0$ at temperatures ranging from 723 to 823 K. The absence of the load transfer at the temperatures under consideration remains to be clarified, independently of whether the creep behaviour is or is not associated with the true threshold stress.

To conclude the present section, Fig. 15 is presented illustrating the spectrum of rate controlling deformation mechanisms identified in the temperature interval 623–948 K. The figure does not need any further comment.

5. Summary and conclusions

In the present paper, results of investigations of creep behaviour in an Al-8.5Fe-1.3V-1.7Si alloy reinforced with 15 vol. % silicon carbide particulates – an Al-8.5Fe-1.3V-1.7Si-15SiC$_p$ composite – are reported and analysed. The creep is investigated at ten temperatures ranging from 623 to 948 K using the isothermal constant stress creep test technique. At temperatures 623, 673 and 723 K the measured minimum creep strain rates cover seven orders of magnitude. The creep is associated with the true threshold stress decreasing with increasing temperature more quickly than the shear modulus of the composite matrix. The creep strain rate is matrix lattice diffusion controlled and the true stress exponent of minimum creep strain rate is close to 5. The creep is interpreted in terms of athermal detachment of dislocations from the incoherent, predominantly $Al_{12}(Fe,V)_3Si$ phase particles in the composite matrix.

At temperatures 773, 798 and 823 K (the measured creep strain rates cover six orders of magnitude) the true threshold stress is not observed. The true activation energy is higher than the activation enthalpy of lattice diffusion in the composite matrix, the true stress exponent increases with increasing stress from about 5 at the lowest stresses up to about 40. The creep is interpreted in terms of the

thermally activated detachment of dislocations from the incoherent $Al_{12}(Fe,V)_3Si$ phase particles.

At temperatures ranging from 873 to 948 K the true threshold stress reappears. However, its origin is different from that at temperatures 623–723 K. The true activation energy of plastic strain is close to the activation enthalpy of grain boundary diffusion and the true stress exponent is close to 2.5. The creep at these temperatures is interpreted in terms of superplasticity.

The observed very high values of the apparent activation energy as well as of the apparent stress exponent under condition of the true threshold behaviour are discussed taking into account load transfer effect. It is shown that the "true threshold stress effect" is more important than the "load transfer effect". The load transfer effect under conditions, when the true threshold stress is absent, is also discussed.

Acknowledgements

Two of the authors (J. Č. and K. K.) thank the Grant Agency of the Academy of Sciences of the Czech Republic for financial support under Grant No. S204 1001. S. J. Z. thanks for support from The University of Electro-Communications, Tokyo, Japan. The assistance of Ms. Eva Najvarová in manuscript preparation is gratefully acknowledged.

REFERENCES

[1] CARREÑO, F.—GONZÁLES-DONCEL, G.—RUANO, O. A.: Mater. Sci. Eng., *A164*, 1993, p. 216.
[2] CARREÑO, F.—RUANO, O. A.: Acta Mater., *46*, 1998, p. 159.
[3] PENG, L. M.—ZHU, S. J.—WANG, F. G.—CHEN, H. R.—MA, Z. Y.: J. Mater. Sci. A, *33*, 1998, p. 5643.
[4] PENG, L. M.—ZHU, S. J.—MA, Z. Y.—BI, J.—CHEN, H. R.—WANG, F. G.: Mater. Sci. Eng., *A259*, 1999, p. 25.
[5] CARREÑO, F.—RUANO, O. A.: Metall. Mater. Trans. A, *30A*, 1999, p. 371.
[6] ZHU, S. J.—KUCHAŘOVÁ, K.—ČADEK, J.: Metall. Mater. Trans. A, *31A*, 2000, p. 2229.
[7] LLOYD, D. J.: Int. Mater., *39*, 1994, p. 1.
[8] PENG, L. M.—ZHU, S. J.—MA, Z. Y.—BI, J.—CHEN, H. R.—WANG, F. G.: J. Mater. Sci. Technol., *6*, 1998, p. 527.
[9] ZHU, S. J.—PENG, L. M.—MA, Z. Y.—BI, J.—WANG, F. G.—WANG, Z. G.: Mater. Sci. Eng., *A215*, 1996, p. 120.
[10] NARDONE, V. C.—PREWO, K. M.: Scr. Metall., *20*, 1986, p. 43.
[11] DRAGONE, T. L.—NIX, W. D.: Acta Metall. Mater., *38*, 1990, p. 1941.
[12] SHI, N.—BOURKE, M. A. M.—ROBERTS, J. A.—ALLISON, J. E.: Metall. Mater. Trans. A, *28A*, 1997, p. 2741.
[13] LI, Y.—NUTT, S. R.—MOHAMED, F. A.: Acta Mater., *45*, 1997, p. 2607.
[14] LI, Y.—LANGDON, T. G.: Metall. Mater. Trans. A, *29A*, 1998, p. 2523.
[15] ČADEK, J.—ZHU, S. J.—MILIČKA, K.: Mater. Sci. Eng., *A248*, 1998, p. 65.
[16] ČADEK, J.—ZHU, S. J.—MILIČKA, K.: Mater. Sci. Eng., *A252*, 1998, p. 1.
[17] ARZT, E.—WILKINSON, D. S.: Acta Metall., *34*, 1986, p. 1893.

[18] ARZT, E.—RÖSLER, J.: Acta Metall., *36*, 1988, p. 1053.
[19] ČADEK, J.—KUCHAŘOVÁ, K.—ZHU, S. J.: Mater. Sci. Eng., *A283*, 2000, p. 172.
[20] BIRD, J. E.—MUKHERJEE, A. K.—DORN, J. E.: Correlation between high-temperature creep behaviour and structure. In: Quantitative relations between properties and microstructure. Eds.: Brandon, D. G., Rosen, A. Jerusalem, Israel University Press 1969, p. 255.
[21] ČADEK, J.—OIKAWA, H.—ŠUSTEK, V.: Mater. Sci. Eng., *A190*, 1995, p. 9.
[22] ČADEK, J.—KUCHAŘOVÁ, K.—MILIČKA, K.—ZHU, S. J.: Kovove Mater., *37*, 1999, p. 213.
[23] LUNDY, T. S.—MURDOCK, J. F.: J. Appl. Phys., *33*, 1962, p. 1671.
[24] KOCKS, U. F.: Philos. Mag., *13*, 1966, p. 541.
[25] PARK, K. T.—MOHAMED, F. A.: Metall. Mater. Trans. A, *26A*, 1995, p. 3119.
[26] MOHAMED, F. A.: Mater. Sci. Eng., *A245*, 1998, p. 242.
[27] ČADEK, J.—KUCHAŘOVÁ, K.—ŠUSTEK, V.: Scr. Mater., *40*, 1999, p. 1269.
[28] ZHU, S. J.—PENG, L. M.—ZHOU, Q.—MA, Z. Y.: To be published; see also ref. 22.
[29] ČADEK, J.—KUCHAŘOVÁ, K.—ZHU, S. J.: Mater. Sci. Eng., *A297*, 2001, p. 176.
[30] RÖSLER, J.—ARZT, E.: Acta Metall. Mater., *38*, 1990, p. 671.
[31] ČADEK, J.—KUCHAŘOVÁ, K.—BŘEZINA, J.—ŠUSTEK, V.: Acta Technica CSAV, *46*, 2001, p. 15.
[32] ORLOVÁ, A.—ČADEK, J.: Acta Metall. Mater., *40*, 1992, p. 1865.
[33] MA, Z. Y.—TJONG, S. C.: Mater. Sci. Eng., *A287*, 2000, p. 5.
[34] KAUR, J.—GUST, W.: Fundamentals of Grain and Interphase Boundary Diffusion. Stuttgart, Ziegler Press 1998, p. 300.
[35] GUST, W.—MAYER, S.—BÖGER, A.—PREDEL, B.: J. Physique C4, *46*, 1985, p. 537.
[36] LANGDON, T. G.: Acta Mater., *42*, 1994, p. 2437.
[37] KIM, W. J.—YEON, J. H.—SHIN, D. H.—HONG, S. H.: Mater. Sci. Eng., *A269*, 1999, p. 142.
[38] MABUCHI, M.—HIGASHI, K.—LANGDON, T. G.: Acta Metall. Mater., *42*, 1994, p. 1739.
[39] LI, Y.—LANGDON, T. G.: Acta Mater., *46*, 1998, p. 3939.
[40] ČADEK, J.: Creep in Metallic Materials. Amsterdam, Elsevier 1988.
[41] KELLY, A.—STREET, K. N.: Proc. Roy. Soc. London, *A238*, 1972, p. 267.
[42] KELLY, A.—STREET, K. N.: Proc. Roy. Soc. London, *A238*, 1972, p. 283.
[43] LI, Y.—LANGDON, T. G.: Acta Mater., *46*, 1998, p. 3937.
[44] LI, H.—LI, J. B.—KANG, Z. G.—WANG, Z. G.: J. Mater. Sci. Lett., *15*, 1996, p. 616.

Received: 24.1.2001